Smart Transformer-based Medium Voltage Grid Support by Means of Active Power Control

Stefano Giacomuzzi, *Student Member, IEEE*, Marius Langwasser, *Student Member, IEEE*, Giovanni De Carne, *Member, IEEE*, Giuseppe Buja, *Life Fellow, IEEE*, Marco Liserre, *Fellow, IEEE*

***Abstract*—In the last decades the voltage regulation has been challenged by the increase of power variability in the electric grid, due to the spread of non-dispatchable generation sources. This paper introduces a Smart Transformer (ST)-based Medium Voltage (MV) grid support by means of active power control in the ST-fed Low Voltage (LV) grid. The aim of the proposed strategy is to improve the voltage profile in MV grids before the operation of On-Load Tap Changer in the primary substation transformer, which needs tens of seconds. This is realized through reactive power injection by the AC/DC MV converter and simultaneous decrease of the active power consumption of voltage-dependent loads in ST-fed LV grid, controlling the ST output voltage. The last feature has two main effects: the first is to reduce the active power withdrawn from MV grid, and consequently the MV voltage drop caused by the active current component. At the same time, higher reactive power injection capability in the MV converter is unlocked, due to the lower active power demand. As result, the ST increases the voltage support in MV grid. The analysis and simulation results carried out in this paper show improvements compared to similar solutions, i.e. the only reactive power compensation. The impact of the proposed solution has been finally evaluated under different voltage-dependence of the loads in the LV grid.**

***Index Terms*—Smart Transformer, Solid State Transformers, Load Control, Voltage Support.**

I. Introduction

THE voltage control has always been a challenge in distribution grids with power utilities involved in keeping the voltage within an allowable range to ensure good power quality to the customers. The primary reason of voltage sags is traditionally due to electric faults, but also the Distributed Generation (DG) plays an important role. In fact, in the last years the deep penetration of Renewable Energy Sources (RESs) in the electric grid has exacerbated this issue, introducing high variability in power availability, because of their intermittent power production, which causes voltage fluctuations along the distribution grid. Even if the DG presence contributes in decreasing the voltage drop along the line, on the other side a sudden and unexpected DG disconnection can generate undervoltage condition, as well as an over production can yield an equally undesired overvoltage situation [1], [2].

The prevailing solution to compensate voltage fluctuations stands on the On-Load Tap Changer (OLTC) in the primary substation transformer, which gears the tap ratio to change the voltage of all the downstream customers [3], [4]. However, the OLTC action suffers from sluggish dynamics (a tap switch every tens of seconds) and a limited number of daily switches.

An alternative approach to achieve fast dynamics consists in the reactive power injection by power electronics equipment. Several equipment has been proposed [5], where the most common are Static Compensators (STATCOMs) and Dynamic Voltage Restorers (DVRs) [6], [7]. STATCOMs and DVRs are generally employed in critical buses of the distribution grids, performing a decentralized voltage support with respect to an OLTC [8], [9]. On the other side, the drawbacks of the OLTC can be minimized, if coordinated with the equipment injection reactive power, to reduce the tap changer switching [10], [11]. Since in the distribution grids the R/X ratio is much higher than in the transmission ones, the active power has strong impact on the voltage support. For this reason, Battery Energy Storage Systems (BESSs) are used to support the voltage in addition to primary frequency regulation services [12].

In the last years, the Smart Transformer (ST) concept has been proposed as central control point in the distribution grid: the ST is a power electronics-based Medium Voltage/Low Voltage (MV/LV) transformer which does not just replace the conventional transformer, but it exploits its dynamic functionalities to offer services to the grid, improving its management [13]-[16]. Among these services, the ST can work similarly to a STATCOM in MV grid, providing voltage support by reactive power injection [17].

This paper presents a ST-based voltage support in MV grids by means of voltage-dependent loads. In case of MV voltage fluctuation, the ST MV converter injects reactive power to support the voltage. If the ST works close to maximum power, its ampacity constraints the reactive power injection. Thus, the ST LV converter decreases the active power consumption of voltage-dependent loads by controlling the ST-fed LV grid voltage, employing the On-Line Load Control (OLLC) strategy [18]. Since MV lines have non-negligible resistive component, the active current reduction improves the ST voltage support

[1]The research leading to these results has been funded by the German Federal Ministry of Education and Research (BMBF) within the Kopernikus Project ENSURE "New ENergy grid StructURes for the German Energiewende" (03SFK1I0 and 03SFK1I0-2), and by the Ministry of Science, Research and the Arts of the State of Baden-Württemberg Nr. 33−7533−30−10/67/1.

Stefano Giacomuzzi and Giuseppe Buja are with the Department of Industrial Engineering, University of Padova, Padova, Italy, email: stefano.giacomuzzi@studenti.unipd.it.

Marius Langwasser, and Marco Liserre are with the Chair of Power Electronics, Kiel University, Kiel, Germany, e-mail: mlan@tf.uni-kiel.de.

Giovanni De Carne is with the Institute for Technical Physics, Karlsruhe Institute of Technology, Karlsruhe, Germany, e-mail: giovanni.carne@kit.edu.

effectiveness for two reasons: i) reduces the voltage drop in the line [19], and ii) unlocks further reactive power injection capability in the ST MV converter.

In detail, the paper is organized as follows: Section II briefly reviews the ST concept and its basic control operations. Section III presents the on-line load sensitivity identification approach [20] and introduces the proposed ST-based voltage support strategy. Section IV demonstrates in a simplified grid the benefit of the proposed voltage support approach, with both theoretical analysis and simulation of a simplified MV grid. In Section V, the validation of the proposed strategy is performed using a coupled IEEE 34-bus test feeder (MV grid) [21] and CIGRE microgrid (LV grid) [22] in order to verify the proposed method performance in realistic grid conditions. Section VI analyzes the impact of the approach under variable ST-fed load sensitivities. Finally, Section VII is dedicated to conclusions.

II. Background

The ST is a power electronics-based transformer, interfacing the MV and LV distribution grids, that aims at increasing their controllability and providing services. Despite the initial higher investment, the ST can bring economic benefit to the grid operators. As demonstrated in the LV-ENGINE project [17], the ST can reduce investment costs from £60m by 2030 up to £500m by 2050.

A. Smart Transformer Concept

The ST is usually structured with a 3-stage topology (Fig. 1): a MV front-end converter, a DC/DC stage, and the LV back-end converter. The MV front-end converter has the tasks to balance the MV DC link voltage, control the active current flow, and to inject reactive current in the MV grid upon request. It can be implemented either as central control which manages the RESs connected in the MV grid, or as local control exploiting the measurements in the ST substation. The latter scheme is adopted in this work. The capability of the reactive power injected in MV through the control of reactive current component is determined by the ST size. Since the ST priority is to properly feed the LV ST-fed grid according to the active power demand of the loads, the reactive power available for the MV injection is calculated as

$$Q_{ST,max} = \pm\sqrt{S_{ST,r}^2 - P_{ST}^2} \tag{1}$$

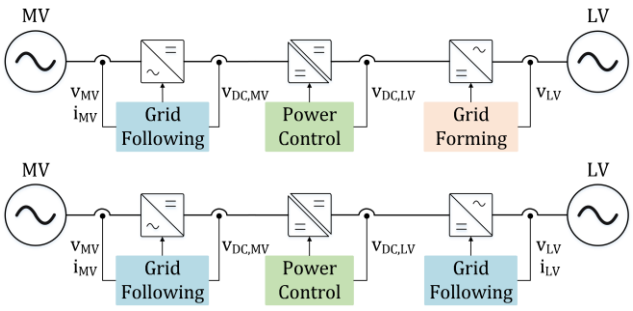

Fig. 1. Smart Transformer concept: grid-forming control of LV grids (figure above), and grid-following control (figure below).

TABLE I. Real MV grid load sensitivities

Load type	Equivalent k_p	Reference
Residential (summer / winter)	0.9 / 1.7	[23]
Commercial (summer / winter)	0.5 / 0.8	[23]
MV aggregated load	1.35	[24]
Primary substations	1.5	[27]

where $S_{ST,r}$ and P_{ST} are the rated value and the active power absorbed by the ST, respectively. With the assumption of a lossless ST, the latter coincides with the total ST-fed LV grid active power requested by the loads. To be noted that the reactive power injection in LV grid is independent from the MV grid, due to the presence of the DC-links. The galvanic insulation and the voltage transformation are guaranteed by the DC/DC converter. Although an external low frequency conventional transformer can offer both insulation and voltage transformation, the ST usually employs a high-frequency transformer (i.e., 10kHz), in order to reduce the weight and size impact in the MV/LV substation. The DC/DC stage controls the power flow between the MV and LV DC link, regulating the LV DC voltage at the nominal level. The low voltage back-end converter can have two control possibilities, depending on the LV grid configuration. If the grid is radial, where the ST acts as main voltage source, the LV converter operates as grid-forming, controlling the voltage waveform in amplitude, frequency and phase. In the case that the ST is connected in parallel with another grid-forming unit (e.g., parallel connection with a conventional transformer), the LV converter control switches to grid-following mode, where it controls the active and reactive power injection in the grid. In this work, the ST LV converter operates in grid-forming mode.

B. ST-based On-Line Load Controller

Varying actively the voltage amplitude, the ST can shape the load consumption of the connected voltage-dependent loads [19]. The aggregate load in LV grid has been found in literature to be dependent from the supply voltage. This dependency generally is affected by the composition of the aggregated load and the loading conditions, such as weather, season or day-time [24], [25], thus it cannot be known a-priori. To find this dependency, an exponential load model is assumed

$$P_{LV} = P_{LV,0}\left(\frac{V_{LV}}{V_{LV,0}}\right)^{k_p} \tag{2}$$

where P_{LV} and $P_{LV,0}$ are the active power of the whole ST-fed LV grid when is applied either the voltage V_{LV} or $V_{LV,0}$ by the ST, respectively. The subscript 0 stands for the nominal value of the referred quantity. The exponent k_p is equal to the active power load sensitivity to the voltage. Considering small variations of both P_{LV} and V_{LV} from their nominal value, the load sensitivity can be obtained from (2) as

$$k_p = \frac{\Delta P_{LV}/P_{LV,0}}{\Delta V_{LV}/V_{LV,0}} \tag{3}$$

As seen in literature from in-field [25] and experimental analysis, the load sensitivity at the primary substation results to behave between constant current ($k_p = 1$) and constant impedance ($k_p = 2$) load [26]. Both industry survey and measurements (summarized in Table I) have been conducted to obtain the equivalent sensitivity of real medium voltage power systems loads, which are aggregated from hundreds or thousands of individual appliances connected to the same substation.

In the ST-fed LV grid the value of k_p is evaluated through an on-line approach by applying a ramp variation of the ST output voltage and subsequently measuring the active power consumption, as described in [20]. As can be noted in Fig. 2, this sequence can be repeated at constant time intervals, e.g. every hour or 10 minutes, in order to update the value of k_p, which follows the changes in the LV grid.

Once the load sensitivity is known, the ST can exploit this information to apply a controlled voltage variation in the LV grid, knowing in advance the power change. As it has been demonstrated in [18], this approach leads to an error in the few percent range, that is acceptable for these applications. A similar method is the so-called Conservation Voltage Reduction (CVR). In this method the energy consumption in the grid is reduced by lowering the voltage into the lower half of the tolerance band by means of OLTCs [28]. Nevertheless, there are several differences between CVR and OLLC. First of all, the ST allows the control of V_{LV} through a closed loop rather than in open loop such as it occurs for the abovementioned methods. Another notable difference is that with CVR the power reduction subsequent to voltage depends on k_p off-line estimation, based on statistics data; on the opposite, in OLLC the desired power reduction is implemented with accuracy, through the real time evaluation of k_p.

The ST modifies its output voltage according to the desired load variation ΔP^*_{LV}.The OLLC is realized setting a new voltage reference given by

$$V^*_{LV} = V_{LV0}\left(1 + \frac{\Delta P^*_{LV}}{P_A k_{pA} + P_B k_{pB} + P_C k_{pC}}\right) \qquad (4)$$

where k_{pA}, k_{pB}, k_{pC} and P_A, P_B, P_C are respectively the load sensitivities and LV active power consumption of each phase at the voltage V_{LV0} and $P_A + P_B + P_C = P_{LV,0}$. Considering a balanced three-phase system where the load sensitivity is the same for each phase and is equal to k_P, and $P_A = P_B = P_C = P_{LV,0}/3$, the voltage reference can be calculated as follows

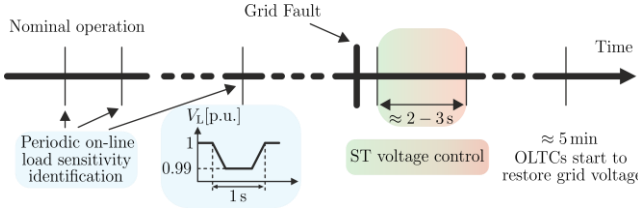

Fig. 2. ST voltage support approach timeline.

$$V^*_{LV} = V_{LV0}\left(1 + \frac{\Delta P^*_{LV}}{P_{LV,0} k_p}\right) \qquad (5)$$

In this work a balanced system is assumed, thus (5) is utilized for the implementation of OLLC.

III. ST-Based Voltage Support by Means of Voltage-Dependent Loads

Transmission lines have mainly inductive behavior, since the resistive part is negligible compared to the reactive one. This leads to the well-known active power/angle and reactive power/voltage relations, where the reactive power influences the grid voltage. Nevertheless, this assumption is only partially valid with MV lines. The cable size is smaller with respect to HV cables, and so is the ratio between cable inductance and resistance. The impact of reactive current is higher for inductive lines, while, with a mainly resistive line, the active power has larger influence on the voltage. It is common knowledge that the resistance/reactance ratio R/X for MV lines is around 1. For these reasons, both active and reactive power have to be controlled to make the voltage support in MV grids more effective during faults.

The proposed ST-based voltage support consists of two control layers, which set the reference quantities for the control of the front-end and the back-end converter, respectively. In the first layer, the ST behaves as any distributed generation resource, injecting capacitive reactive power in the MV grid, in order to sustain the voltage. In case this reactive power is not sufficient, and the ampacity of the MV converter is reached, the ST switches to the second control layer. Here the ST decreases the LV demand consumption by means of the OLLC approach. This leads to two positive effects: a decrease of the MV line drop and more room for the MV converter to inject reactive power. The overall control structure is shown in Fig. 3, and described in details below.

A. MV front-end converter controller

The control scheme of the ST MV converter is depicted in Fig. 4. The Park transformation is used to transform the sinusoidal output quantities into direct ones through the matrix $\boldsymbol{T_{dq}}$. The outer loop on the d-axis regulates the MV DC link voltage, generating the current reference $i_{ST,d}$ which is then compared with the d-component of the current measured on the

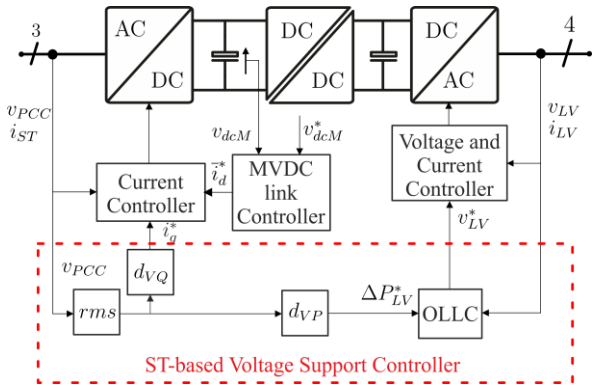

Fig. 3. ST control scheme and Voltage Support Controller (in red). The DC/DC controller is omitted to increase the figure readability.

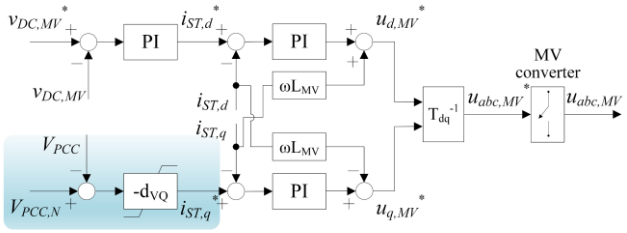

Fig. 4. MV converter control scheme.

output filter. The error is sent to a Proportional Integral (PI) controller) and its output is added to the cross term $\omega L_{MV} i_{ST,q}$ to give the d-component of the voltage reference for the inverter. The controllers of the two loops are tuned accordingly to the technical optimum (inner loop) and symmetrical optimum (outer loop) techniques. Note that L_{MV} is the inductance of the output filter. In parallel, the q-axis MV controller has the task to control the reactive injection. The generation of the MV q-axis current reference, relevant to this work, is highlighted in blue in Fig. 4, while the description of the inner current loop is omitted because analogous to the d-axis current controller. If the voltage in the MV grid drops, the MV converter of the ST can initially support the voltage injecting reactive power. The ST measures the voltage V_{PCC} at the ST input on MV side and sends the measurements to the reactive power controller. In this application, a droop function with coefficient d_{VQ} has been adopted to receive as input the voltage deviation and to give as output the new MV q-axis current set-point:

$$d_{VQ} = \frac{I^*_{ST,q}}{\Delta V_{PCC}} \tag{6}$$

where $\Delta V_{PCC} = V_{PCC} - V_{PCC,N}$ is the deviation of MV from its nominal value. Nevertheless, the reactive injection of MV converter is limited by (1). It follows that when ST is withdrawing active power close to its nominal rating, the amount of available reactive power at the MV converter is inadequate to achieve satisfying voltage support to the MV grid. It is important to remind that, in order to contain the initial investment, the ST is designed for the nominal load, avoiding costly oversizing of components. Consequently, it usually has small margin to inject reactive power in the MV grid.

B. LV back-end converter controller

To overcome this drawback, the reactive power injection is coordinated with a second layer control, that regulates the active power consumption in LV grid by means of OLLC approach. The voltage measurement V_{PCC} is thus sent in parallel

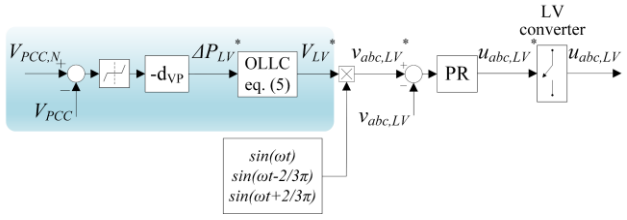

Fig. 5. LV converter control scheme.

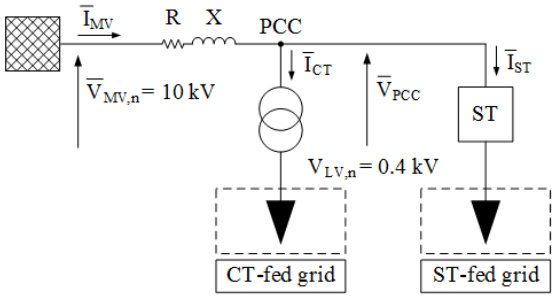

Fig. 6. Circuital scheme of the study case.

to the OLLC block, where a gain d_{VP} links the voltage drop in the MV grid to the power variation set-point ΔP^*_{LV} to apply in the LV grid. The OLLC, knowing in advance the LV grid load sensitivity k_p, varies the voltage set-point V^*_{LV} of the ST-fed LV grid according to (5). The control scheme of the LV converter is shown in Fig. 5, where the generation of the amplitude V^*_{LV} is highlighted in blue. A dead band is inserted in order to enable the OLLC only for MV deviations larger than ±5%, since for smaller fluctuations the load reduction is considered as not necessary.

The droop coefficient of the active power control loop is defined as follows

$$d_{VP} = \frac{\Delta P^*_{LV}}{\Delta V_{PCC}} \tag{7}$$

At MV reduction corresponds a LV power reduction, and vice versa. It results that higher droop coefficients lead to higher power reduction/increase. By combining (7) with (5), the active power droop coefficient can be rewritten as

$$d_{VP} = k_p \frac{P_{LV,0}}{V_{LV,0}} \frac{\Delta V^*_{LV}}{\Delta V_{PCC}} \tag{8}$$

where $\Delta V^*_{LV} = V^*_{LV} - V_{LV0}$. The generation of the voltage references $v_{abc}{}^*$ is then achieved by the product of the obtained V^*_{LV} with three sinewaves rotating at the angular frequency ω, each one lagging $(2/3)\pi$ respect to the other. The control scheme is completed with the voltage control loop where a Proportional Resonant (PR) controller gives as output the references for the LV converter. Note that the *abc*-frame is implemented in the LV controller of the ST, because it is possible to provide unbalance voltage to the LV grid if

TABLE II. BASE PARAMETERS

Parameters	Value
V_B	10 kV
S_B	1 MVA

TABLE III. OPERATING CONDITIONS OF THE STUDY CASE

Quantity	Symbol	Value [pu]
CT Active Power	P_{CT}	0.38
ST Active Power	P_{ST}	0.38
ST Power rating	$S_{ST,r}$	0.5
Line impedance	Z	0.08

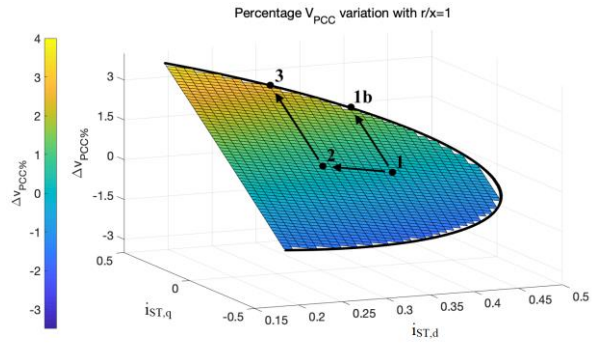

Fig. 7. Percentage voltage variation of PCC as a function of ST reactive and active current for $R/X = 1pu$.

requested. However, the alternative choice to implement a dq-frame controller for the LV converter is also possible, without affecting the generality of the proposed control methodology.

From the point of view of the MV support, the advantage of the OLLC application is twofold: i) the active current component flowing in the MV grid decreases, and so does the voltage drop along the line; ii) the reduced ST active power absorption from MV grid enables more room in the ST MV converter. Subsequently, the reactive power injection can further increase, improving the voltage support. It is worth to underline that the resistive-inductive nature of the MV grid is fundamental for the active power compensation, since its impact on pure inductive lines would be negligible.

IV. Analytical and Simulation Results of the Proposed Control Strategy

In Fig. 6 the circuital scheme of a simplified grid used for analytical purpose is presented with phasor quantities. A MV distribution grid supplies a ST-fed LV grid, with the rest of the grid consisting of an aggregate load fed by a Conventional Transformer (CT). Since the ST and the CT are connected to the same PCC, the CT-fed LV grid benefits from ST voltage support action. The base values of the circuit are listed in Table II, whilst Table III describes the steady-state working values adopted for the study case. Both the ST- and CT-fed grids are absorbing active power equal to 0.38pu. R and X are the MV line resistance and reactance; V_{PCC} is the rms value of PCC voltage. The total MV line current $\bar{I}_{MV}$ is given by the sum of $\bar{I}_{ST}$ and $\bar{I}_{CT}$, which are the currents flowing in the ST- and CT-fed grid, respectively. In nominal operating conditions, the ST is set to absorb only active power, with its delivered reactive power equal to zero, thus reducing the inductive current flowing across the line, which contributes in dropping the voltage. A power factor cosφ=0.9 is assumed for the aggregate load fed by the CT, according to minimum limit usually allowed by dispositions of the Distributor System Operator.

The voltage support offered by the ST is temporary, before the OLTC at the HV/MV substation gears the tap changer to increase the line voltage. The ST can provide a faster response in terms of voltage support, thanks to its power electronics nature. The subsequent OLTC intervention aims to restore the nominal voltage conditions at the PCC: when this is achieved, the ST mediation is no more required. In this Section the improvement in the PCC voltage are shown, comparing the proposed active-reactive compensation with no compensation at all and the only reactive one.

TABLE IV. Simulation Results of the Study Case

Magnitude	Control technique	Steady-state value before the event	Steady-state value after the event
ST MV converter voltage in p.u.	No Q, no OLLC	**0.967**	**0.886**
	d_{VQ} = 20, no OLLC	**0.975**	**0.896**
	d_{VQ} = 20, d_{VP} = 2	**0.975**	**0.904**
	d_{VQ} = 20, d_{VP} = 4	**0.975**	**0.908**
	d_{VQ} = 20, d_{VP} = 8	**0.975**	**0.913**
ST active power in p.u.	No Q, no OLLC	**0.42**	**0.42**
	d_{VQ} = 20, no OLLC	**0.42**	**0.42**
	d_{VQ} = 20, d_{VP} = 2	**0.42**	**0.386**
	d_{VQ} = 20, d_{VP} = 4	**0.42**	**0.361**
	d_{VQ} = 20, d_{VP} = 8	**0.42**	**0.325**
ST reactive power in p.u.	No Q, no OLLC	**0**	**0**
	d_{VQ} = 20, no OLLC	**-0.147**	**-0.147**
	d_{VQ} = 20, d_{VP} = 2	**-0.147**	**-0.233**
	d_{VQ} = 20, d_{VP} = 4	**-0.147**	**-0.274**
	d_{VQ} = 20, d_{VP} = 8	**-0.147**	**-0.322**

A. Analytical evaluation

The advantage to use the ST-based voltage support in MV grids by means of voltage-dependent loads is evaluated quantitatively in Fig. 7, where the ST MV converter ampacity equal to 0.5pu (observable from Table III) is shown in solid black line. To perform this analysis, the data in Table II and Table III have been used, with the line ratio $R/X = 1$, typical of MV lines. In Fig. 7, the subscripts a and r identify the active and reactive components of the ST current absorbed by MV converter, considering the PCC voltage as reference. If the ST is working close to maximum capability, the reactive power that can be injected is limited and the voltage support capability is restricted, even if strongly dependent on the R/X ratio. For instance, this concept has been further clarified with an example in Fig. 7: Point 1 represents the nominal working point, where ST is withdrawing only the active power necessary to feed the ST-fed LV grid, without any exchange of reactive power with the upstream MV grid. The ST current components are $I_{ST,d}$=0.38pu and $I_{ST,q}$=0pu. When the ST requires to inject reactive current keeping on withdrawing the same active power, its maximum reactive current component is limited to $I_{ST,q}$=0.32pu, identified as point 1b, leading to a PCC voltage increase of about 1.5%. If the OLLC decreases the ST-fed LV grid power of 20%, and thus the ST active current $I_{ST,d}$ decreases up to Point 2, i.e., $I_{ST,d}$=0.3pu, the voltage increase in MV is 0.5%. By decreasing the active current flowing in the MV converter, there is further room for reactive current increase. In this condition, the converter limits the reactive current to $I_{ST,q}$=0.4pu as shown from point 3. The total voltage boost in this case is 2.64%, with an improvement of more than

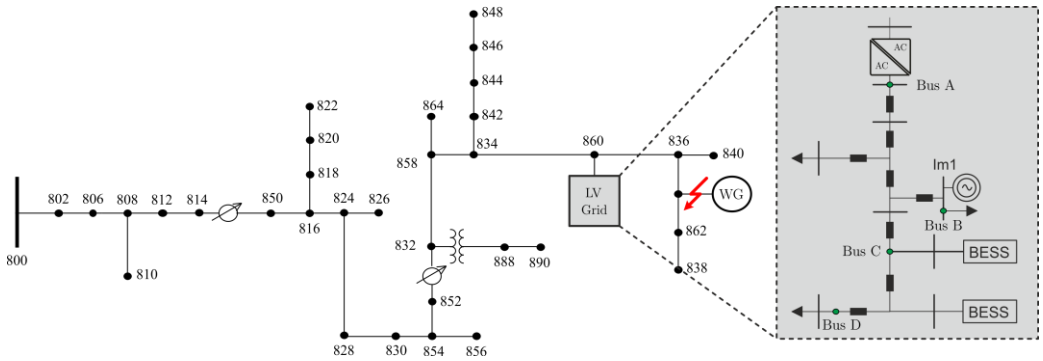

Fig. 8. Combined MV grid (IEEE 34-bus test feeder [21]) and LV grid (CIGRE Microgrid benchmark [22]) used in this validation. The two distribution grid are interfaced by means a ST at bus 860. The critical load is connected between bus 634 and bus 860.

1% compared to the pure reactive injection detected in point 1b. This example explains practically the main advantage of adopting a ST for reactive power control, instead of alternative solutions such as STATCOM.

It is worth reminding that the ST does not act as any controllable energy sources, where the active power injection can be freely dispatched. The ST active power demand depends only on the connected loads; thus, the active power consumption cannot be shaped directly, but it has to be influenced by other variables, i.e. voltage.

B. Simulation tests

The performance of the proposed ST-based voltage support has been demonstrated in this section by means of simplified simulations, based on the scheme shown in Fig. 6. The simulations have been carried in PLECS/Matlab environment and they have the only purpose to show the performance of the proposed approach during a voltage drop in the MV grid at 0.95pu for 300ms. This may represent a typical voltage sag during faults, with the following fault clearance by protections. The load sensitivity k_p is assumed to be 1 for the aggregate load of the ST-fed LV grid and 0 for the one of the CT-fed LV grid (considered as worst case), corresponding to constant current and constant power load, respectively.

The following three control modes are considered:

- No reactive power compensation, where the ST works as constant power load seen from MV grid.
- Reactive power compensation, where the ST injects reactive power to support the MV grid voltage (d_{VQ}=20pu).
- ST-based voltage support by means of voltage-dependent loads, where the ST decreases the ST-fed LV grid power consumption. In this case three droop gains are assumed:
  - $d_{VP} = 2pu$
  - $d_{VP} = 4pu$
  - $d_{VP} = 8pu$

In Table IV, the effectiveness of the ST-based voltage support by means of voltage-dependent loads is shown. In case of no voltage support (identified as no Q, no OLLC), the voltage drops at 0.88pu during the disturbance. If the reactive power control is assumed, the voltage drop is limited below 0.9pu, showing minimal results. The proposed ST-based voltage support strategy is instead able to restore the voltage at the PCC of the critical load above 0.9pu, while it reaches about 0.913pu in case of d_{VP}=8pu. The advantage in decreasing the active

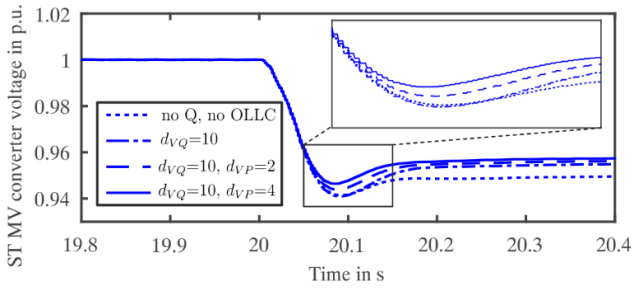

Fig. 9. ST MV converter voltage V_{PCC}: no reactive power and no OLLC action (dotted line), only reactive power injection and no OLLC (dashed-dotted line), 10% load control (dashed line), and 20% load control (solid line).

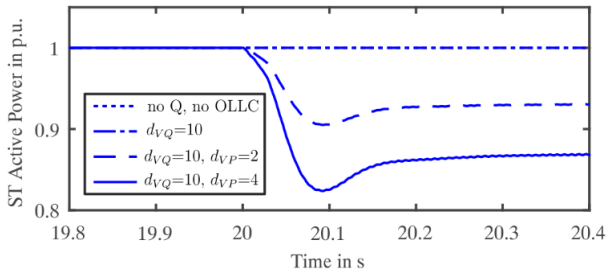

Fig. 10. ST active power: no reactive power and no OLLC action (dotted line), only reactive power injection and no OLLC (dashed-dotted line), 10% load control (dashed line), and 20% load control (solid line).

TABLE V. STEADY-STATE RESULTS OF THE STANDARD GRID BENCHMARK

Magnitude	Control technique	Steady-state value before the event	Steady-state value after the event
ST MV converter voltage in p.u.	No Q, no OLLC	**1**	**0.948**
	d_{VQ} = 10, no OLLC	**1**	**0.954**
	d_{VQ} = 10, d_{VP} = 2	**1**	**0.956**
	d_{VQ} = 10, d_{VP} = 4	**1**	**0.957**
ST active power in p.u.	No Q, no OLLC	**1**	**1**
	d_{VQ} = 10, no OLLC	**1**	**1**
	d_{VQ} = 10, d_{VP} = 2	**1**	**0.93**
	d_{VQ} = 10, d_{VP} = 4	**1**	**0.872**

power consumption is also shown in Table IV, where the ST active and reactive power are described, respectively. It can be seen that the reactive power injection in the case without OLLC is limited to 0.147pu by the converter ampacity, while when the OLLC is implemented, the capability to inject reactive power increases from 0.23pu up to 0.32pu, according to the droop coefficient d_{VP}.

V. Validation with a Standard Grid Benchmark

To validate the effectiveness of the proposed ST-based voltage support strategy with respect the simple injection of reactive power in the MV grid, the ST has been implemented in a PSCAD simulation, connecting the IEEE 34-bus test feeder [21] and the CIGRE Microgrid benchmark [22] (Fig. 8). The overall system works at 60Hz and balanced three-phase voltage of 10kV and 0.4kV, respectively. The ST is installed at the bus 860, and the ST-fed LV grid includes 2 BESSs, as described in [22], and an induction machine of 8 kW installed at bus B.

At the 20th second, the wind turbine connected between bus 836 and bus 862, due to an internal fault, disconnects, and the system is short of 650 kW of active power. This causes a sudden voltage drop at the ST busbar as can be seen in the dotted lines in Fig. 9. As possible solution, the ST can inject only reactive power (d_{VQ}=10) in the MV grid to support the voltage (dashed-dotted lines). Despite some improvements in steady state, where the voltage recovers of 1%, the reactive power impact during the transient is limited due to the ST reactive power control dynamics, which are not deeply examined because out of the scope of the paper. If the reactive power injection is coordinated with the OLLC action, the ST is able not only to partially recover the voltage in steady state (1.5%), but also to limit the voltage and power drop during the transient. Table V reports the steady-state values for the voltage of the ST MV converter and the ST active power, which indicates the active power reduction in the ST-fed LV grid. Two cases have been considered for the OLLC (Fig. 10): in one case d_{VP}=2, meaning that 5% of voltage drop at the busbar corresponds 10% of power reduction of the ST-fed LV grid (large-dashed lines); in the other case, d_{VP}=4, that corresponds to 20% power reduction for 5% voltage drop (solid lines). Instead to reach a negative peak below 0.94pu in case of no ST support, the negative peak reaches about 0.95pu.

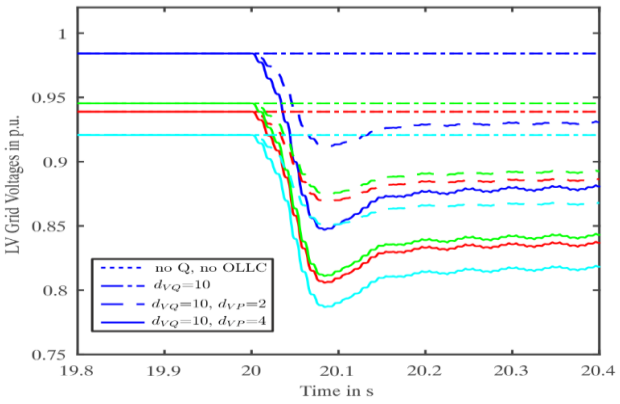

Fig. 11. ST-fed LV grid voltage profile: no reactive power and no OLLC (dotted line), only reactive power injection (dashed-dotted line), 10% load control (dashed line) and 20% load control (solid line). The plotted buses are Bus A, B, C and D, respectively in blue, green, red and cyan line.

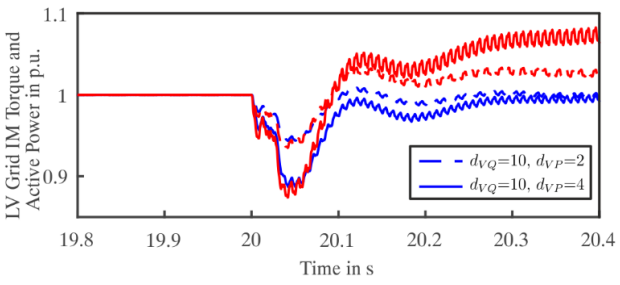

Fig. 12. Induction machine power (blue line) and torque (red line), in case of: 10% load control (dashed line), and 20% load control (solid line).

Following the MV grid voltage reduction, the OLLC reduces the voltage in the ST-fed LV grid. With respect to the cases without OLLC action, the voltage in LV grid can drop up to 0.85pu in the furthest bus from the ST in the "d_{VP}=2" case, and up to 0.78pu in the "d_{VP}=4" case, as shown in Fig. 11, where the two lines representing the cases without OLLC overlap. Though these values can affect the quality of service in the LV grid, it must be noted that the ST OLLC action is a temporary measure while the HV/MV OLTC transformer intervenes to increase the voltage. As consequence of the voltage decrease, the power of the ST-fed LV grid changes, decreasing of 7% in the "d_{VP}=2" case and of 13% in the "d_{VP}=4" case.

A. Impact of the control on LV loads

Low voltage condition generated by OLLC in LV grid can affect the induction machines connected, leading them to stall [29]. In Fig. 12, the active power (blue lines) and torque (red lines) of the 8 kW induction machine connected to bus B of ST-fed grid are shown. It can be noted that in both OLLC cases, the induction machine undergoes a drop in torque and power, while regaining in 200ms the previous active power, and showing a small increase in the torque value (about 5-7%) in the new steady-state conditions. This demonstrates that for such values of voltage reduction induced by OLLC, the induction machines do not take the risk of stalling. It shall be remembered that due to the temporary nature of this control, the voltage in the ST-fed LV grid will be restored after the HV/MV OLTC action.

TABLE VI. Simulation Results for Different ST-fed Load Sensitivities

Magnitude	Active power load sensitivity to voltage (K_P)	Steady-state value before the event	Steady-state value after the event
ST MV converter voltage in p.u.	0.5	**0.975**	**0.899**
	1	**0.975**	**0.904**
	2	**0.975**	**0.914**
ST active power in p.u.	0.5	**0.42**	**0.41**
	1	**0.42**	**0.386**
	2	**0.42**	**0.319**
ST reactive power in p.u.	0.5	**-0.147**	**-0.183**
	1	**-0.147**	**-0.233**
	2	**-0.147**	**-0.328**

VI. Variable ST-fed load sensitivity

The effectiveness of the proposed strategy depends on the load sensitivity to voltage variation in the ST-fed LV grid. To analyze different load conditions, the simulations performed in Section IV have been repeated with the results shown in Table VI considering different load sensitivities of the ST-fed LV grid: k_p=0.5, k_p=1, k_p=2. These values respect conditions under different integration of constant power loads in the LV grid, as they are the power electronics-based appliances.

As can be seen, the more sensitive are the loads, the more voltage support capability the ST can offer. In case of constant impedance loads (k_p=2), the PCC voltage recovery during the disturbance increases of 2% compared to the case of more constant power loads (k_p=0.5). The reason can be easily found in Table VI, where for the same LV reduction, the active power decreases of 0.01pu with k_p=0.5 and of 0.1pu with k_p=2, to whom corresponds an increase in reactive power injection availability from 0.036pu to 0.181pu, respectively.

VII. Conclusions

Disturbances, such as faults or RESs variability, can affect the voltage quality in distribution lines. The ST offers the possibility to support the voltage profile during first moments after large disturbances, before OLTC reaction, mitigating the voltage sags in the MV grid. The ST, on the opposite of solutions such as STATCOM, not only injects reactive power in MV grid, but also contributes to the voltage support acting on the ST-fed LV grid consumption. Controlling the voltage amplitude, the ST is able to interact with the voltage-sensitive loads and to decrease the LV grid power consumption. This leads to two main advantages: the reduction of the active current voltage drop in the MV grid, and more room available in the ST MV converter to inject higher reactive power. As shown in the simulation results and in the PSCAD validation with complex MV and LV grids, a single ST is able to achieve up to 2% voltage improvement during voltage drops, corresponding at the double with respect to the only reactive power injection case, and with a limited impact in the ST-fed loads.

References

[1] Institute for Energy Research, “Germany’s green energy destabilizing electric grids”, posted Jan. 23, 2013 [Online]. Available: http://www.instituteforenergyresearch.org/2013/01/23/germanys- green-energy-destabilizing-electric-grids/

[2] Math Bollen, “The Smart Grid – Adapting the power system to new challenges”, Synthesis Lecturers on Power Electronics, Series Editor: Jerry Hudgins, Morgan & Claypool Publishers, Chapter 2, 2011.

[3] K. M. Muttaqi, A. D. T. Le, M. Negnevitsky, and G. Ledwich, “A co-ordinated voltage control approach for coordination of OLTC, voltage regulator, and DG to regulate voltage in a distribution feeder” *IEEE Trans. Ind. Appl.*, vol. 51, no. 2, pp.1239–1248, Mar./Apr. 2015.

[4] R. Echavarria, A. Claudio and M. Cotorogea, “Analysis, Design, and Implementation of a Fast On-Load Tap Changing Regulator,” *IEEE Trans. Power Electron.*, vol. 22, no. 2, pp. 527-534, Mar. 2007.

[5] J. Dixon, L. Moran, J. Rodriguez and R. Domke, “Reactive Power Compensation Technologies: State-of-the-Art Review,” *Proc. IEEE*, vol. 93, no. 12, pp. 2144-2164, Dec. 2005.

[6] M. Molinas, J. A. Suul and T. Undeland, “Low Voltage Ride Through of Wind Farms With Cage Generators: STATCOM Versus SVC,” *IEEE Trans. Power Electron.*, vol. 23, no. 3, pp. 1104-1117, May 2008.

[7] J. G. Nielsen, M. Newman, H. Nielsen and F. Blaabjerg, “Control and testing of a dynamic voltage restorer (DVR) at medium voltage level,” *IEEE Trans. Power Electron.*, vol. 19, no. 3, pp. 806-813, May 2004.

[8] A. Jain, K. Joshi, A. Behal, and N. Mohan, “Voltage regulation with STATCOMs: Modeling, control and results,” *IEEE Trans. Power Del.*, vol. 21, no. 2, pp. 726–735, Apr. 2006.

[9] C. Wessels, F. Gebhardt and F. W. Fuchs, “Fault Ride-Through of a DFIG Wind Turbine Using a Dynamic Voltage Restorer During Symmetrical and Asymmetrical Grid Faults,” *IEEE Trans. Power Electron.*, vol. 26, no. 3, pp. 807-815, Mar. 2011.

[10] A. Samadi et al., “Coordinated active power-dependent voltage regulation in distribution grids with PV systems,” *IEEE Trans. Power Del.*, vol. 29, no. 3, pp. 1454–1464, Jun. 2014.

[11] X. Guo and W. Chen, “Control of multiple power inverters for more electronics power systems: A review,” *CES Trans. Elect. Mach. Syst.*, vol. 2, no. 3, pp. 255-263, Sep. 2018.

[12] F. Ciccarelli, D. Iannuzzi, K. Kondo and L. Fratelli, “Line-Voltage Control Based on Wayside Energy Storage Systems for Tramway Networks” *IEEE Trans. Power Electron.*, vol. 31, no. 1, pp. 884-899, Jan. 2016.

[13] S. Bhattacharya, “Transforming the Transformer,” *IEEE Spectrum*, vol. 54, no. 7, pp. 38-43, July 2017.

[14] M. Liserre, G. Buticchi, M. Andresen, G. De Carne, L. F. Costa, and Z. X. Zou, “The smart transformer: Impact on the electric grid and technology challenges,” *IEEE Ind. Electron. Mag.*, vol. 10, pp. 46–58, Summer 2016.

[15] F. Ruiz, M. A. Perez, J. R. Espinosa, T. Gajowik, S. Stynski and M. Malinowski, “Surveying Solid-State Transformer Structures and Controls: Providing Highly Efficient and Controllable Power Flow in Distribution Grids,” *IEEE Ind. Electron. Mag.*, vol. 14, no. 1, pp. 56-70, Mar. 2020.

[16] https://www.spenergynetworks.co.uk/pages/lv_engine.aspx

[17] A. Milczarek and M. Malinowski, “Comparison of Classical and Smart Transformers Impact on MV Distribution Grid,” *IEEE Trans. Power Del.*, vol. 35, no. 3, pp. 1339-1347, Jun. 2020.

[18] G. De Carne, G. Buticchi, M. Liserre and C. Vournas, “Load Control Using Sensitivity Identification by Means of Smart Transformer,” *IEEE Trans. Smart Grid*, vol. 9, no. 4, pp. 2606-2615, Jul. 2018.

[19] S. Giacomuzzi, G. Buja, G. De Carne, and M. Liserre, “Application of Smart Transformer Load Control to mitigate Voltage Fluctuations in Medium Voltage Networks,” in Proc. IEEE Power Energy Soc. Gen. Meeting, Portland, Aug. 2018, pp. 1-5.

[20] G. De Carne, M. Liserre and C. Vournas, “On-Line Load Sensitivity Identification in LV Distribution Grids,” *IEEE Trans. Power Syst.*, vol. 32, no. 2, pp. 1570-1571, Mar. 2017.

[21] Distribution Test Feeders, IEEE/PES. (2015, Aug.). 34-bus Feeder. [Online]. Available: http://ewh.ieee.org/soc/pes/dsacom/testfeeders/index.html.

[22] “Benchmark system for network integration of renewable and distributed energy resources c06.04.02,” CIGRE, Tech. Rep., 2014.

[23] IEEE Task Force on Load Representation for Dynamic Performance, “Load representation for dynamic performance analysis (of power systems),” *IEEE Trans. Power Syst.*, vol. 8, no. 2, pp. 472–482, May 1993.

[24] D. P. Stojanovic, L. M. Korunovic, and J. Milanovic, “Dynamic load modelling based on measurements in medium voltage distribution network,” *Electric Power Syst. Res.*, vol. 78, no. 2, pp. 228–238, 2008.

[25] A. Ballanti, L. N. Ochoa, K. Bailey and S. Cox, “Unlocking New Sources of Flexibility: CLASS: The World's Largest Voltage-Led Load-Management Project,” *IEEE Power Energy Mag.*, vol. 15, no. 3, pp. 52-63, May-Jun. 2017.

[26] J. V. Milanovic, K. Yamashita, S. Martinez Villanueva, S. Z. Djokic, and L. M. Korunovic, “International industry practice on power system load modeling,” *IEEE Trans. on Power Syst.*, vol. 28, no. 3, pp. 3038–3046, Aug. 2013.

[27] G. Delille, L. Capely, D. Souque, and C. Ferrouillat, “Experimental validation of a novel approach to stabilize power system frequency by taking advantage of load voltage sensitivity,” in 2015 IEEE Eindhoven PowerTech, Jun. 2015, pp. 1–6.

[28] Z. Wang and J. Wang, “Review on implementation and assessment of conservation voltage reduction,” *IEEE Trans. Power Syst.*, vol. 29, no. 3, pp. 1306–1315, May 2014.

[29] D. Zhang and T. Liu, “Effects of voltage sag on the performance of induction motor based on a new transient sequence component method,” *CES Trans. Elect. Mach. Syst.*, vol. 3, no. 3, pp. 316-324, Sep. 2019.